

# AUTONOMOUS ORBIT DETERMINATION FOR SPACECRAFTS BASED ON THE TIME-OF-ARRIVAL OF SOLAR RADIATION

Jingshi Tang<sup>(1)</sup>, Feng Yan<sup>(2)</sup>, and Lin Liu<sup>(3)</sup>

<sup>(1)</sup>*School of Astronomy and Space Science, Nanjing University, 163 Xianlin Dadao, Nanjing, 210023, +86-25-89683269, jstang@nju.edu.cn*

<sup>(2)</sup>*School of Electronic Science and Engineering, Nanjing University, 163 Xianlin Dadao, Nanjing, 210023, +86-25-89681090, fyan@nju.edu.cn*

<sup>(3)</sup>*School of Astronomy and Space Science, Nanjing University, 163 Xianlin Dadao, Nanjing, 210023, +86-25-83595440, lliu@nju.edu.cn*

**Abstract:** *We consider using the Sun for the autonomous orbit determination (AOD), replacing the x-ray pulsars. The solar radiation received by the Earth satellites can be much stronger than that of the strongest x-ray pulsars and is therefore easier to be detected and utilized. Since the radiation emitted by the Sun is no longer periodic, the radiation profile cannot be modeled but has to be measured on site. We include multiple spacecrafts in the scheme so the differenced observations can be obtained between the spacecrafts. We discuss the correlation of the profiles at different spacecrafts to obtain the time difference of arrival (TDOA). We simulate with a piece of actual solar radiation to show whether the different profiles received by the spacecrafts can be correlated to determine the actual TDOA of the same wavefront. Then we assess the performance of AOD with such differenced observations. We would simulate with some spacecrafts in medium Earth orbit (MEO). Besides only using TDOA, we also include the satellite-to-satellite tracking (SST) measurements in the simulation. We expect that combining both SST and TDOA measurements can reduce the limitation and increase the accuracy and stability of this AOD scheme.*

**Keywords:** *Autonomous Orbit Determination, Time-of-arrival, Solar Radiation.*

## 1. Introduction

Using x-ray pulsars for autonomous satellite navigation and orbit determination dates back to the 1970s. After the discovery of the pulsars in the 1960s, scientists proposed that periodic x-ray pulsars can serve as a beacon in the space for the autonomous satellite navigation [1]. The satellite observes the radiation profile of the x-ray pulsars and convert it to the Solar System Barycenter (SSB) system. By comparing the observed profile with the "standard profile" established using accumulated ground observations, it is possible that we obtain the phase differences and thus the barycentric distance of the satellite in the direction of the pulsar. The measurement is connected to the barycentric system and is therefore possible for the satellite to autonomously determine its own orbit.

This approach was initially proposed decades ago, yet it still remains a theory. In the recent decade, scientists keep working on the theory and some of the latest and advanced results can be found in [2, 3]. However, autonomous orbit determination (AOD) using x-ray pulsars is hardly implemented in space, not to mention any practical applications. The most famous test in space so far is the Unconventional Stellar Aspect (USA) onboard Advanced Research and Global Observation Satellite (ARGOS) [4].

The major fact that limits the application of AOD using x-ray pulsars is the weak x-ray radiation in the Earth vicinity or the Solar System. In [3], Hanson et al. carefully analyzed the AOD error using x-ray pulsars. First, they chose the pulsars with certain pulsated fraction as the candidate for AOD application. Under this condition, only the Crab pulsar (B0531+21) has a count rate above  $1 \text{ ph/cm}^2/\text{sec}$  in the  $2 - 10 \text{ keV}$  band, while the count rates of other candidates are much smaller than 1, by 3 – 4 orders of magnitude.

The time-of-arrival (TOA) error is also quantitatively estimated. With Monte-Carlo simulation and model analysis [3], it is found that for the Crab pulsar, when the product of area and integral time ( $S \cdot \tau$ ) is around  $10 - 100 \text{ m}^2 \cdot \text{sec}$ , the TOA  $1\sigma$  error is about  $1 - 10 \mu\text{s}$ . For the TOA error to reduce to  $0.1 - 1 \mu\text{s}$ ,  $S \cdot \tau$  has to be as large as  $10^3 - 10^4 \text{ m}^2 \cdot \text{sec}$ . It means that the onboard sensor with a  $1 \text{ m}^2$  detecting area has to observe the Crab pulsar for  $100 \text{ sec}$  to obtain a  $1 \mu\text{s}$  TOA accuracy and for approximately 3 hours for a  $0.1 \mu\text{s}$  TOA accuracy. This is just the ideal case for the brightest candidate pulsar near the Earth, and the situation is much worse for other candidates. For B1821-24 [3], a  $1 \text{ m}^2$  sensor has to observe for about  $10^5 \text{ sec}$  or over 27 hours only to obtain a  $0.1 \mu\text{s}$  TOA accuracy.

For this reason, although some x-ray pulsars have nice periodicity, the weak flux in the Earth vicinity greatly limits the practical application. Recently Sheikh et al. start to focus on other aperiodic radiation sources with higher flux yet using similar TOA differenced measurements [5, 6]. However, it is to be noted that they are still focusing on the deep space high energy celestial bodies such as aperiodic quasar [5] or even gamma-ray burst (GRB) [6]. Although they comparatively exceed x-ray pulsars in terms of local flux, their fluxes remain low. For GRB, the burst characteristics (unpredictable object and time with a short burst duration) basically concludes its infeasibility in real missions.

Since 2014, we have been working to use the Sun, instead of other deep space celestial sources, for AOD. Below, we show our preliminary surveys and simulations results. We show that the local flux is steadily higher than the Crab pulsar by about 3 order of magnitude. Using the currently available scientific data as template, we can simulate profiles of higher temporary resolution and manage to successfully correlate the Solar radiation profiles and obtain the time difference of arrival (TDOA), if the errors of the onboard clock and sensors are reasonably small enough. In such circumstances, the AOD based on TDOA and satellite-to-satellite tracking (SST) measurements can be successfully completed with comparable accuracy to the original observations.

## 2. Solar Radiation

So far, there are several solar telescopes operating in space. Here we choose the GOES satellites from the National Oceanic and Atmospheric Administration (NOAA). The GOES series are chosen for two reasons. One is that it has good coverage in the x-ray band. The other is that the GOES satellites have consistent designs or specifications in the same generation, so observations between different such satellites can be compared. Current operational satellites in orbit are GOES-N (#13), GOES-O (#14) and GOES-P (#15), which belong to the same generation. They can generate x-ray images of the Sun in the  $0.05 - 0.4 \text{ nm}$  ( $3.1 - 24.8 \text{ keV}$ ) and  $0.1 - 0.8 \text{ nm}$  ( $1.55 - 12.4 \text{ keV}$ ) bands. The imager onboard the GOES-NOP satellites is the Solar X-ray Imager (SXI), which is basically

a solar telescope in the x-ray band [7] with a geometric area of  $726 \text{ mm}^2$  [8].

Currently GOES-15 is the primary working satellite, while GOES-13 is also observing in orbit. Therefore it is possible that we compare the x-ray profiles between different satellites with the same specification. With the scientific data released by NOAA, we show the  $0.1 - 0.8 \text{ nm}$  profile obtained by GOES-13 and GOES-15 on July 6 2015 and July 15 2015. Given that the photon count is used in AOD for correlation, we plot the profile of photon counts in Fig. 3.

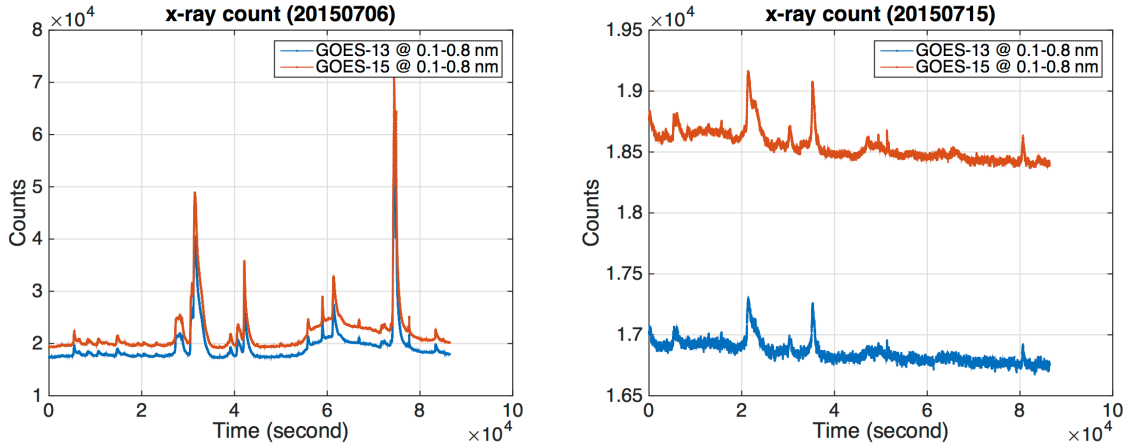


Figure 1. Photon counts of solar x-ray radiation in  $0.1 - 0.8 \text{ nm}$  band, received by GOES-13 and GOES-15 on July 6 2015 (left) and July 15 2015 (right)

Given the scientific objective of the satellites, although GOES-13 and GOES-15 are equipped with the telescopes of the same specification, it is likely that they are not calibrated between each other and thus the bias between the profiles could exist. Nevertheless, the profiles observed by both satellites are apparently quite close. We expect that if the profiles are calibrated and recorded with high temporal resolution, we can correlate both profiles and obtain high accuracy TDOA measurement.

On the other hand, the photon count in Fig. 3 is around  $2 \times 10^4$ . With a mirror area of  $7.26 \text{ cm}^2$  and a temporal resolution of around  $2 \text{ sec}$  of the scientific data, the solar x-ray flux in the  $0.1 - 0.8 \text{ nm}$  band is about  $1 - 2 \times 10^3 \text{ ph/cm}^2/\text{sec}$ , which is much larger than that of the Crab pulsar, the brightest x-ray pulsar candidate for AOD.

### 3. Preliminary AOD Scheme

Unlike using x-ray pulsars, multiple satellites have to be included to utilize solar x-ray radiation for differenced measurement. Fig. 2 shows the scheme using two satellites. The satellites are called Server and Client, representing their respective roles in the approach. This scheme can be extended to a satellite constellation with sufficient operational and backup satellites to sustain the autonomous operation of the system. A preliminary scheme is planned as follows.

1. All the satellites in the constellation continuously and simultaneously receive the solar x-ray radiation profiles, and record TOA with high accuracy and high temporal resolution;

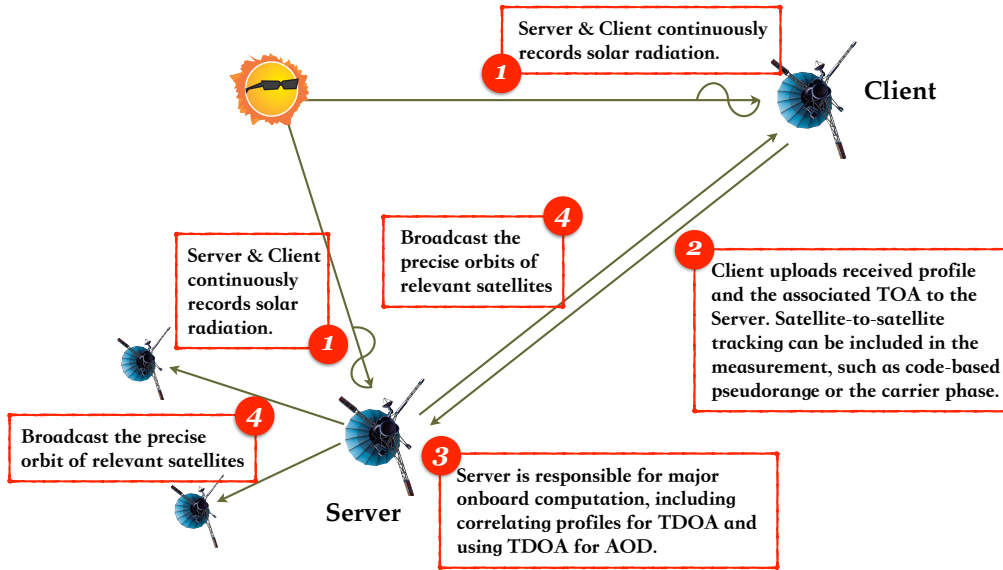


**Figure 2. AOD Scheme using solar x-ray radiation**

2. The Clients upload their received profiles with the TOA to its associated Server. Since inter-satellite communication is essential in the scheme, including SST measurement is a natural complement to enhance the observation geometry and the orbit determination stability;
3. AOD computation is completed onboard Servers. The computations include i) converting Client-based TOA to the Server frame, ii) correlating the profiles from the Client and the Server to obtain the TDOA series, and iii) using TDOA measurements for AOD. If SST is included, Servers are also responsible to compute pseudorange from the code or the carrier phase;
4. Servers also need to distribute the precise orbits of the relevant satellites, so all the satellites can have their ephemerides regularly updated.

To help understand the scheme, we explain some of the details below.

- Servers play the key role in the AOD scheme, taking up almost all the AOD computations. In real implementation, we expect that there should be multiple servers. Both servers and clients share the same design and specification, only assigned with different roles in the system. The distributed design allows the satellites to switch between different roles in times of need and enhances the stability and robustness of the navigation constellation;
- SST is not compulsory to ensure AOD. Using TDOA is already sufficient to maintain the autonomous operation, yet it is subject to the observation geometry and the orbit determination (OD) accuracy may be compromised by observation errors. Accurate SST measurement is planned for future navigation system such as GPS or Beidou and is a helpful complement to enhance current AOD scheme;
- The AOD system can be deployed in current satellite navigation system in the 12-hour medium Earth orbit (MEO), but other orbits can also be considered, such as Beidou's 24-hour geostationary orbit (GEO) and inclined geosynchronous orbit (IGSO). The accuracy and stability of the AOD system benefit from a variety of orbit geometries.

## 4. Simulation Tests

The simulation tests are twofold. One is the correlation tests using solar x-ray profiles. Assuming appropriate errors in TOA and photon counts, we see if the profiles can be correlated and also if the TDOA between them can be estimated. The other test focuses on the relation between the TDOA errors and AOD accuracy, which can serve as a quantitative guidance in mission design.

### 4.1. Correlation Test

For this test, we use actual solar x-ray photon counts in the  $0.1 - 0.8 \text{ nm}$  band recorded by GOES-15 on July 6 2015. We choose 6 different locations in the profile, including peaks, slopes and flat segments. The segments for correlation tests are selected with both 5-minute and 15-minute spans. Fig. 3 illustrates how we select the segments in the profile. The correlation tests are completed following the steps below.

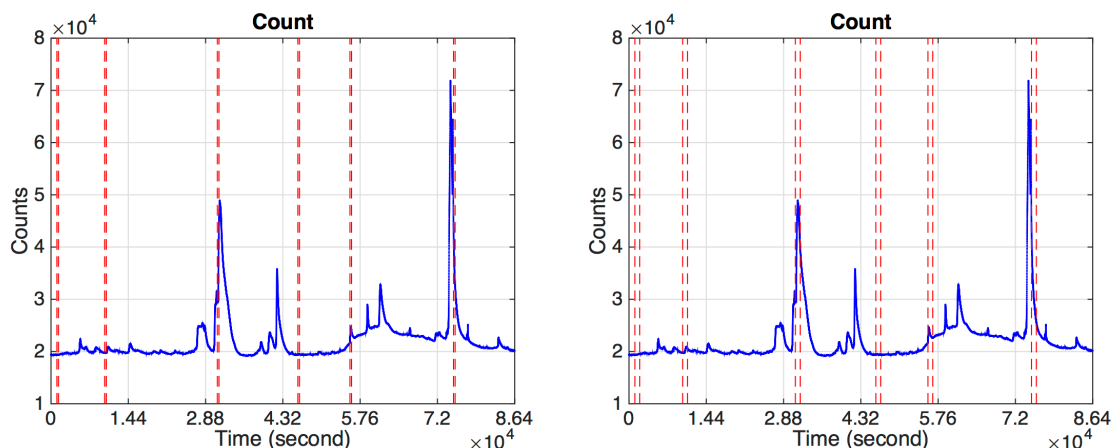


Figure 3. Solar x-ray ( $0.1 - 0.8 \text{ nm}$ ) photon counts received by GOES-15 on July 6 2015. The segments between each pair of red lines are selected for correlation tests, spanning 5 minutes (left) and 15 minutes (right) respectively.

1. For each profile segment, shift it forward by 5 points. With a 2-second temporal resolution, this yields a +10 TDOA *test* segment with respect to the *original* one;
2. Respectively add Gaussian white noise to the test and the original segments. The noises are added to both the recorded TOA (simulating the clock-wise error) and the photon counts (simulating the sensor-wise error), with a zero mean and a standard deviation of  $1 \text{ ms}$  and  $100 \text{ counts}$  respectively;
3. Shift the test segment by the *trial TDOA* from -30 seconds to 10 seconds with a 2-second increment and correlate it with the original one. We compute the correlation coefficient for each trial and find the maximum. The TDOA associated with the maximum correlation coefficient is considered to be the true TDOA;
4. For each segment of either length, we repeat Steps 1~3 for 20 times and estimate the success rate in the Monte-Carlo sense.

The second shift-and-trial step is computed in a symmetric range with respect to the true TDOA. In real scenario, we can estimate possible TDOA range based on a priori satellite orbits and proceed

with the shift-and-trial in that estimated range.

Results show that shifting the test segment by -10 seconds corresponds to the largest correlation coefficients, suggesting that the TDOA values in all tests are correctly estimated to be +10 seconds. Fig. 4 shows the correlation results in one test of the Monte-Carlo simulations. With given clock and sensor errors, we can correctly and unambiguously determine the TDOA.

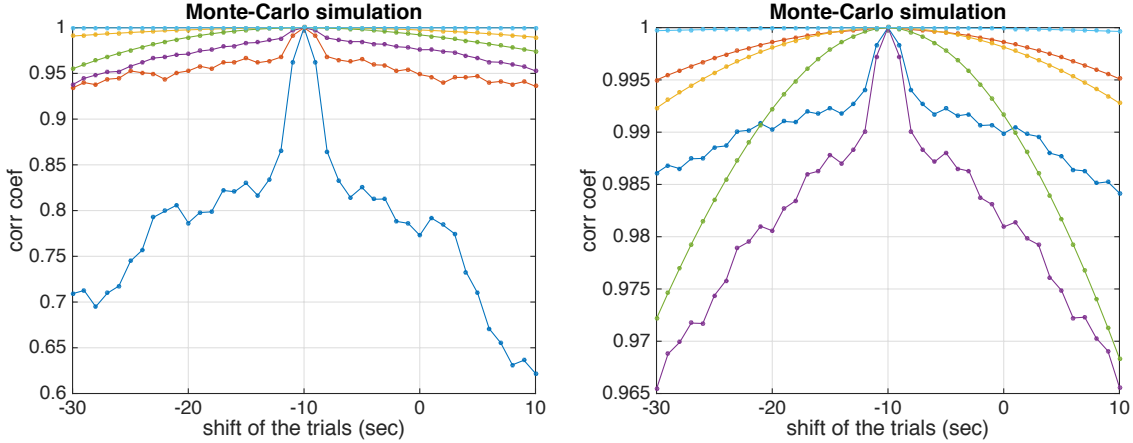


Figure 4. Correlation results of an arbitrary test in the Monte-Carlo simulation, for a 5-minute segment (left) and a 15-minute segment (right) respectively. The  $x$ -axis is the shifted time in the trials and  $y$ -axis is the corresponding correlation coefficient.

Nevertheless, we mention that the difference between the correlation coefficients of different segments is subject to the fluctuation in the photon count. A segment with a sharp peak is obviously more favorable than a smooth slope. In real application, we may additionally evaluate the confidence of the estimated TDOA and discard whose confidence levels are below certain threshold.

## 4.2. OD Test

To utilize the solar x-ray radiation, at least two satellites are needed to accomplish the differenced measurement. Therefore it is natural that we first simulate it using current navigation satellite constellation. In this section, we use the orbits of 4 currently operational Beidou navigation satellites, whose orbits are converted from two-line elements and are listed in Tab. 1. The initial states are given in Keplerian elements, which are the semi-major axis ( $a$ ), the eccentricity ( $e$ ), the orbit inclination ( $i$ ), the right ascension of ascending node ( $\Omega$ ), the argument of perigee ( $\omega$ ) and the mean anomaly ( $M$ ).

Using this setup, we simulate TDOA and SST measurements for 24 hours, between the Server and each one of the Clients. For the initial states of AOD, errors are added to the elements, which are 64 km for  $a$ , 0.01 for  $e$  and  $0^\circ.57$  for  $i, \Omega, \omega$  and  $M$ . We first verify the AOD approach by directly determining the precise initial orbits using original simulated measurements without any observation errors. Results show that with or without complement SST, AOD steadily converges to the precise orbits in Tab. 1. In equivalent distance, the AOD root-mean-square (RMS) is 0.51 m

**Table 1. Initial Keplerian elements and roles of 4 Beidou satellites used in the test**

Role	$a$ (km)	$e$	$i$ ( $^\circ$ )	$\Omega$ ( $^\circ$ )	$\omega$ ( $^\circ$ )	$M$ ( $^\circ$ )
Server	27905.889336	0.00241454	55.757783	83.483234	200.709010	293.952556
Client	27904.978963	0.00275621	55.692578	82.975759	195.093814	226.441172
Client	27903.129427	0.00363606	54.696462	203.139659	161.548723	116.365274
Client	27907.482314	0.00162254	54.808399	202.638547	203.781445	345.208401

using only TDOA and is 0.42  $m$  using TDOA and SST. These results prove that using TDOA is observable for AOD.

For the quantitative guidance in future mission design, we add errors of different levels to the simulated measurements. Then we determine the orbits and look for certain relationship between the observation error and the final AOD error. For both TDOA and SST measurements, we assume zero-mean Gaussian white noise and run 6 groups of tests with different standard deviations listed in Tab. 2. For each group, we run a Monte-Carlo simulation with 100 OD tests, in case of using TDOA only and using TDOA+SST.

**Table 2. Standard deviations ( $1\sigma$ ) of observation errors in the AOD tests**

Group #	1	2	3	4	5	6
$1\sigma$ (ns)	10	50	100	500	1000	5000

To save space, we do not go into the details of the 1200 OD tests, but simply present the statistical accuracy of the  $6 \times 2 = 12$  groups. Fig. 5 shows the AOD accuracy (in RMS) under different TDOA errors. We mention that even in the worst case ( $1\sigma = 5$  ms), most RMS values are close and not very large. However, the mean value can still deteriorate due to some very large RMS values in a small fraction of the tests and is a pessimistic estimate of the overall AOD accuracy. Therefore in Fig. 5, the overall accuracy of each group is represented by the median RMS values, while the largest and smallest RMS values are indicated by the error bars.

Two conclusions can be drawn from this simulation.

1. When the observation error is large (e.g. over 1  $\mu s$ ), the SST measurement is essential to stabilize the AOD performance. Whereas when the observation error is small (e.g. below 1  $\mu s$ ), only using TDOA is sufficient for accurate and stable AOD performance;
2. AOD RMS shows a linear relation with the observation error, with a scale of about 1.4. Although it is obtained using the particular orbits in Tab. 1 and may be subject to the actual constellation, it promisingly suggests that this AOD approach can guarantee equal level of accuracy to the observations.

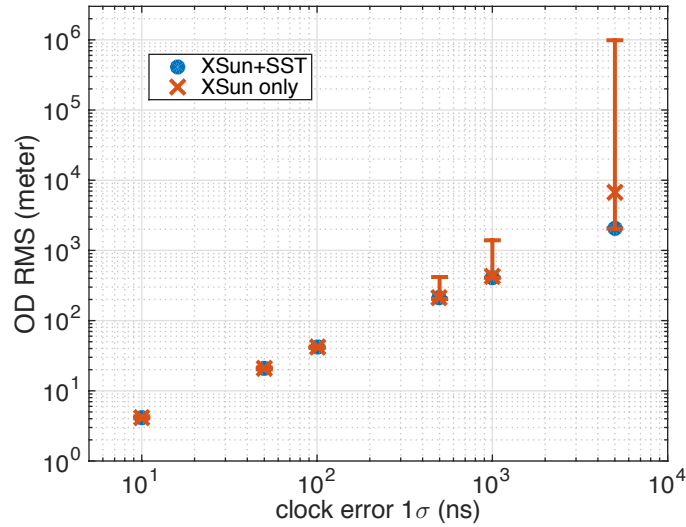


Figure 5. AOD RMS values of all 12 groups of tests. The blue “.” represents the TDOA+SST tests whereas the red “×” the TDOA-only tests. Markers are plotted at the median RMS values and the error bars indicate the error maximum and minimum.

## 5. Conclusion

In this paper, we propose an autonomous orbit determination approach using the differenced measurements of solar x-ray radiation time of arrival. We investigate the solar x-ray radiation in the 0.1 – 0.8 nm band with the scientific data observed by space solar telescope GOES-13 and GOES-15. Compared with the traditional AOD approach using the x-ray pulsars, the local photon flux is 3 orders of magnitude higher. The geometric area of the current GOES-NOP series is 7.26 cm<sup>2</sup>, considerably smaller than those proposed for x-ray pulsars in various literatures, and is of great advantage for real applications.

In the preliminary simulations, we show with the 2-second GOES-15 scientific data that given appropriate observation errors, it is possible that we correlate the photon profiles and obtain the TDOA values. For the AOD tests, we combine the TDOA measurements with intersatellite tracking, based on the real Beidou orbits. Under different error levels, the AOD approach is shown to be promising in terms of both accuracy and stability. A quantitative guidance is thus obtained for the tested Beidou orbits.

## 6. References

- [1] Downs, G. S. “Interplanetary Navigation Using Pulsating Radio Sources.” Tech. Rep. N74-34150, NASA, 1974.
- [2] Sheikh, S. I., Pines, D. J., Ray, P. S., Wood, K., Lovellette, M. N., and Wolff, M. T. “Spacecraft Navigation Using X-ray Pulsars.” *Journal of Guidance Control and Dynamics*, Vol. 29, No. 1, pp. 49–63, 2006.



- [3] Hanson, J., Sheikh, S., Graven, P., and Collins, J. “Noise analysis for X-ray navigation systems.” “Position, Location and Navigation Symposium, 2008 IEEE/ION,” pp. 704–713. 2008.
- [4] Wood, K. S., Kowalski, M., Lovellette, M. N., Ray, P. S., Wolff, M. T., Yentis, D. J., Bandyopadhyay, R. M., Fewtrell, G., and Hertz, P. L. “The Unconventional Stellar Aspect (USA) Experiment on ARGOS.” “AIAA Space 2001 Conference and Exposition,” Paper 2001-4664. 2001.
- [5] Sheikh, S. I., Ray, P. S., Weiner, K., Wolff, M. T., and Wood, K. “Relative Navigation of Spacecraft Utilizing Bright, Aperiodic Celestial Sources.” “ION 63rd Annual Meeting,” Cambridge, Massachusetts, 2007.
- [6] Hisamoto, C. S. and Sheikh, S. I. “Spacecraft Navigation Using Celestial Gamma-Ray Sources.” *Journal of Guidance Control and Dynamics*, Vol. 38, pp. 1765–1774, 2015.
- [7] “GOES-NOP Overview Brochure.”  
Retrieved from [http://sxi.ngdc.noaa.gov/docs/GOES-NOP\\_Brochure\\_40p.pdf](http://sxi.ngdc.noaa.gov/docs/GOES-NOP_Brochure_40p.pdf).
- [8] “GOES-NOP Databook (Chap 6, Rev D).”  
Retrieved from [http://sxi.ngdc.noaa.gov/docs/GOES\\_N\\_Series\\_Databook\\_rev-D\\_ch6\\_SXI.pdf](http://sxi.ngdc.noaa.gov/docs/GOES_N_Series_Databook_rev-D_ch6_SXI.pdf).